

# Insight into protein–protein interactions from analytical ultracentrifugation

Stephen E. Harding<sup>1</sup> and Arthur J. Rowe

National Centre for Macromolecular Hydrodynamics, University of Nottingham, Sutton Bonington, Leicestershire LE12 5RD, U.K.

## Abstract

Analytical ultracentrifugation is a free solution technique with no supplementary immobilization, columns or membranes required, and can be used to study self-association and hetero-interactions, stoichiometry, reversibility and interaction strength across a very large dynamic range (dissociation constants from  $10^{-12}$  M to  $10^{-1}$  M). In the present paper, we review some of the advances that have been made in the two different types of sedimentation experiment – sedimentation equilibrium and sedimentation velocity – for the analysis of protein–protein interactions and indicate how major complications such as thermodynamic and hydrodynamic non-ideality can be dealt with.

## Introduction

Analytical ultracentrifugation [1] is a technique for the analysis of the concentration distribution of a macromolecular solute in solution at high centrifugal field, based upon either how the concentration distribution changes with time (known as sedimentation velocity, SV) or (at relatively lower centrifugal fields) the final steady-state concentration distributions after sedimentation and diffusive forces have come to equilibrium (sedimentation equilibrium, SE). The two methods, possible on the same instrumentation, can provide a powerful and complementary insight into the stoichiometry, reversibility, strength and, in some cases, dynamics of protein–protein interactions and across a wide range of interaction strengths, from very strong (molar dissociation constants  $K_d \sim 10^{-12}$  M) to extremely weak ( $K_d \sim 10^{-1}$  M). In the present paper, we review some of the advances that have been made in the application of these methods to protein–protein interactions and focus on how major complications such as non-ideality (thermodynamic or hydrodynamic) can be dealt with. Choice of the appropriate optical system is important and we consider this first. We then consider SE, how this can be used to provide stoichiometry, reversibility and interaction strength information for both homo- and hetero-associations, and how it is possible to eliminate complications due to thermodynamic non-ideality (arising from co-exclusion and polyelectrolyte effects), an important consideration particularly when trying to characterize weak interactions. We illustrate the application of the method both to strong interactions (a heterodimerization), where non-ideality considerations can be neglected, and to weak interaction between proteins involved in cellular/molecular recognition phenomena. We then consider the application of the SV method, first of all for

the analysis of strong irreversible interactions (illustrated by a protein–glycoprotein mucoadhesive system), and then from sedimentation coefficient distribution analysis the characterization of irreversible antibody associations and reversible associating systems, both protein and carbohydrate in nature.

## Choice of optical system

The ultracentrifuge cell loading concentration selected depends on the strengths of the interactions or potential interactions being probed, and this also has a bearing on the appropriate optical system used. For weak or very-weak interactions ( $K_d 10^{-4}$ – $10^{-1}$  M), higher concentrations (>5 mg/ml) are necessary and for these the Rayleigh interference optical system is most appropriate. For moderate-strength interactions of order  $K_d \sim 10^{-7}$ – $10^{-4}$  M, (0.1–5 mg/ml), either interference optics or UV absorption optics may be appropriate, but for very-strong interactions ( $K_d < 10^{-7}$  M) dye-labelled proteins and fluorescence optics are necessary. SE experiments on a single loading concentration can define a full range of interaction terms (i.e.  $K_d$  and thermodynamic terms), but study of a range of concentrations is needed to provide information about reversibility. With the SV, dynamic information, such as the rate constant  $k_{off}$  ( $s^{-1}$ ), as well as  $K_d$  and hydrodynamic terms may be available.

## Sedimentation equilibrium

SE in the ultracentrifuge is a condition attained when the centrifugal and back-diffusive forces come to thermodynamic equilibrium, yielding a steady-state concentration distribution which is a function of buoyant solute mass and mass distribution, and, for interacting systems, Mass Action parameters such as the equilibrium association constant  $K_a$ , or the equivalent dissociation constant  $K_d$  (usually expressed in molar units). The distribution will also be influenced by thermodynamic non-ideality

**Key words:** analytical ultracentrifugation, non-ideality, protein–protein interaction, sedimentation equilibrium, sedimentation velocity.

**Abbreviations used:** SE, sedimentation equilibrium; SV, sedimentation velocity.

<sup>1</sup>To whom correspondence should be addressed (email [steve.harding@nottingham.ac.uk](mailto:steve.harding@nottingham.ac.uk)).

arising from co-exclusion and polyelectrolyte effects, which, in some cases, under conditions of high dilution are not significant, but otherwise need to be taken into account:

$$c(r) = f(M_b, B, C, K, r) \quad (1)$$

where  $c(r)$  is the concentration at a radial position  $r$  in the ultracentrifuge cell,  $M_b$  is the buoyant molar mass,  $B$  is a measure of the thermodynamic non-ideality (usually one non-ideality coefficient, the 'second' virial coefficient suffices, although sometimes, particularly at higher concentrations, a third coefficient  $C$  is needed). Note that  $B, C \dots$  are called the virial 'coefficients': the products  $BM, CM \dots$  are the 'virial terms', and have simple reciprocal mass concentration units.  $K$  represents the association or dissociation constants (for a simple binary interaction such as a self-association or an  $A + B = AB$ -type interaction, a single constant is appropriate):

$$B = f(\text{excluded volume, charge}) \quad (2)$$

$$K_a = [AB]/([A] \cdot [B]) \quad (3)$$

and  $K_a$  the association constant (in l/mol) =  $1/K_d$ , where  $K_d$  is the dissociation constant.

The buoyant molar mass is given by  $M_b = M(1 - \bar{v}\rho_o)$ , where  $M$  is the molecular mass or molar mass (Da or g/mol),  $\bar{v}$  is the partial specific volume (ml/g) of the solute and  $\rho_o$  is the density of the solvent (g/ml). In a heterogeneous system (e.g., for an interacting system, a mixture of the products and reactants), this will usually be a weight-average  $M_w$ , but can be a z-average  $M_z$  if a special type of optics known as Schlieren or 'refractive index gradient' optics, not currently present on modern ultracentrifuges, is used or the data are manipulated in a particular way. If non-ideality is significant,  $M$  (or  $M_w, M_z$ ) will be an apparent molecular mass  $M_{app}$  ( $M_{w,app}, M_{z,app}$ ). For a monomer-dimer equilibrium, for example, correct to first order in concentration and if virial terms higher than second are ignored,  $B$  is taken to be single-valued and a binomial approximation to incorporate the contribution of  $K_a$  is accepted, then the relationship between the apparent molecular mass as estimated by SE and the total solute concentration  $c$  can be approximated by:

$$(1/M_{w,app}) \approx (1/M_1) + 2(B_{11} - [K_a/M_1^2])c \quad (4)$$

where  $M_1$  is the monomer molecular mass,  $B_{11}$  is the monomer-monomer second virial coefficient (the first virial coefficient is  $1/M_1$ ),  $c$  (g/ml) is the total solute concentration (of monomer and dimer) and the distribution of mass between these two species is given by the Law of Mass Action. A similar relation exists for the apparent z-average molecular mass, except that the coefficient in eqn (4) is 4 and not 2.

The  $c(r)$  against  $r$  distribution (eqn 1) at SE has historically been presented in several exponential- or logarithmic-based forms (for a review, see [2]). One popular exponential form has been given in the widely used NONLIN software [3], which facilitates the estimation of the parameters in eqn (1) by

means of non-linear fitting algorithms. It should be noted that only one, but never both, of the thermodynamic ( $B$  or  $BM$ ) and mass-interactive ( $K_a$ ) terms can be floated in a single fit.

The first example we have chosen involves the definition by this approach of a strong interaction of the  $A + B = AB$  type, the electron-transfer flavoprotein heterodimer ETF, where the association is between one polypeptide chain of  $M \sim 29$  kDa and another of 34 kDa [4]. At the low concentrations employed to study it, one can to a reasonable approximation assume the system to be ideal:  $B_{11} \sim 0$  in eqn (4). For this type of system, an old but valid approach is to define the average molecular mass as a function of concentration, studied over a range in  $c$  where the last mentioned assumption remains valid.

SE here was performed at four different loading concentrations and solute distributions recorded using UV-absorption optics. Three types of analysis were employed. First,  $M_{w,app}$  was measured for each of the four concentrations. Figure 1(a) shows these values obtained using a procedure known as MSTAR [5] (downloadable from <http://www.nottingham.ac.uk/nmh/software>), a procedure particularly suited to the analysis of heterogeneous systems: plots of  $M_{w,app}$  against  $c$  are useful for defining the stoichiometry of the system, in this case clearly a simple  $A + B = AB$  system. Another manipulation is particularly useful for assessing the reversibility of the reaction: the  $c(r)$  against  $r$  data can be transformed into a plot of  $\ln c(r)$  against  $r^2$ , which in turn is transformed into a plot of 'point' average molecular masses or  $M_{w,app}(r)$  against  $c(r)$ . These can then be plotted on the same axes for different loading concentrations. If the system is a genuine reversible equilibrium, then these datasets should overlay and fall on the same  $M_{w,app}(r)$  against  $c(r)$  curve [6]; this was indeed the case for the ETF system (Figure 1b). Finally, one can fit the  $c(r)$  against  $r$  datasets to eqn (1) (Figure 1c), or an equivalent form of this in a procedure known as 'PSI analysis' [7], to estimate  $K_a$  (or  $K_d$ ) (Figure 1d). This demonstration of a strong reversible  $A + B$  interaction proved consistent with the subsequent model of the system based on high-resolution measurements [8].

For weaker interactions, the contribution of thermodynamic non-ideality effects cannot be ignored.

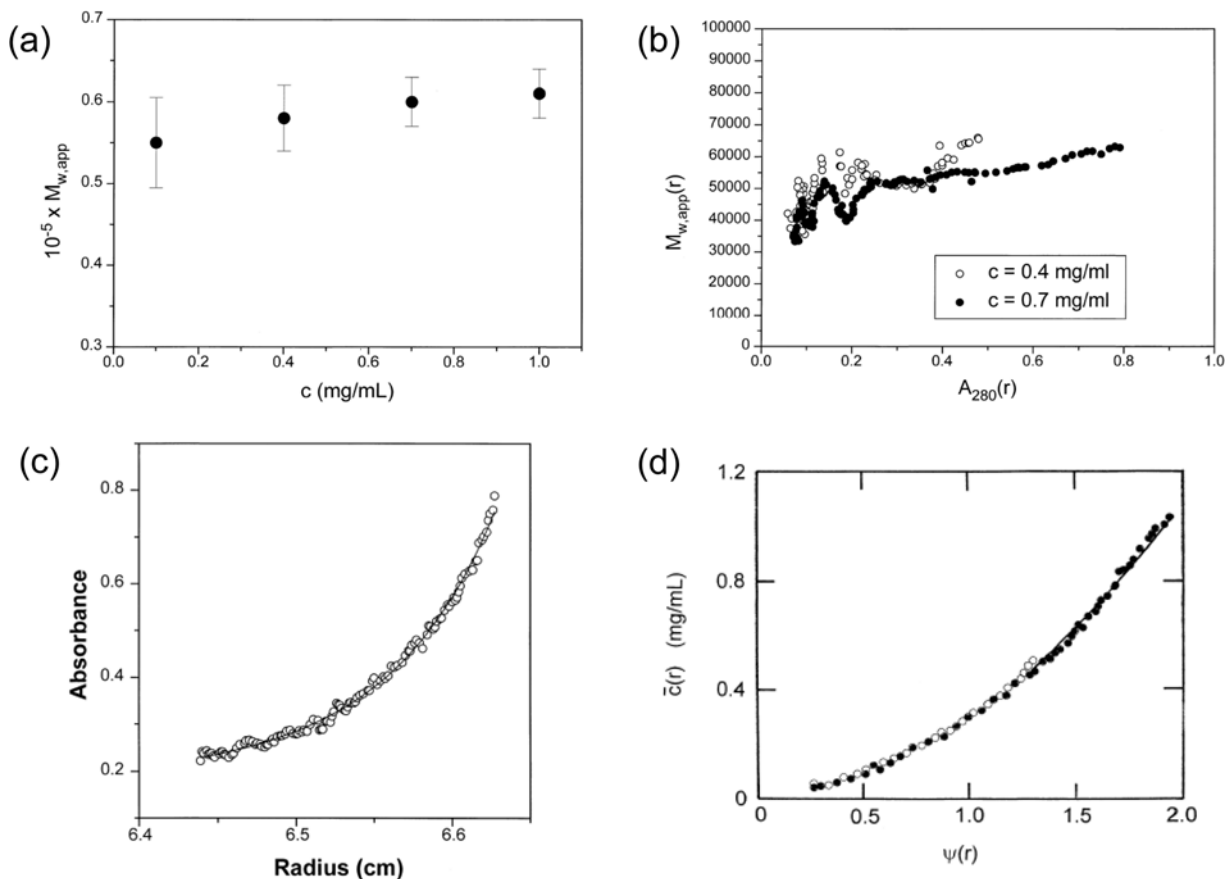
A way of dealing with this problem was introduced in 1999 using a procedure known as COVOL [9,10]. It is based on earlier theory [11] allowing the calculation of the exclusion volume contribution to the second thermodynamic virial coefficient  $B_{ex}$ . To do this, an estimate of the triaxial shape of the monomeric species is required (from for example X-ray crystallography [12]), together with the molecular mass. For the charge or polyelectrolyte contribution to the second thermodynamic virial coefficient  $B_z$ , knowledge of the valency of the protein under the solvent conditions and the ionic strength of the solvent is required:  $B_{11}$  can then be defined as

$$B_{11} = B_{ex} + B_z \quad (5)$$

and no longer has to be regarded as a variable in the analyses for  $K_a$  or  $K_d$ .

**Figure 1 | SE analysis of the heterodimerization of the electron transfer flavoprotein ETF**

The dimerization is of two equimolar components of molecular mass 28 900 and 33 700 kDa respectively. **(a)**  $1/M_{w,app}$  against  $c$  plot for four different cell loading concentrations showing a monomer-dimer system with dimer molecular mass  $\sim 63$  kDa (including FAD and AMP cofactors of collective  $M = 1120$  Da) dissociating at lower concentration ( $M_{w,app}$  is the apparent weight-average molecular mass, averaged over all radial positions in the ultracentrifuge cell from meniscus to cell base). **(b)** Plot of the 'point' apparent mass average,  $M_{w,app}(r)$  evaluated at individual radial positions  $r$  as a function of concentration [expressed as UV-absorbance  $A(r)$  values at 280 nm] at those radial positions. Datasets for two loading concentrations are shown. Within error, they overlap, demonstrating a reversible interaction. **(c)** Modelling the concentration distribution in terms of an ideal dimerization. **(d)** As **(c)**, but in terms of the radial function  $\psi(r)$ . The fitted data in both **(c)** and **(d)** correspond to a  $K_d \sim (1.5 \pm 0.1) \times 10^{-6}$  M, a strong interaction. Again the overlap at two different loading concentrations is commensurate with a reversible association. With kind permission from Springer Science + Business Media: European Biophysics Journal, Low temperature solution behaviour of *Methylophilus methylotrophus* electron transferring flavoprotein: a study by analytical ultracentrifugation, **25**, 1997, pp. 411-416, H. Cölfen, S.E. Harding, E.K. Wilson, N.S. Scrutton and D.J. Winzor, Figures 2-5.



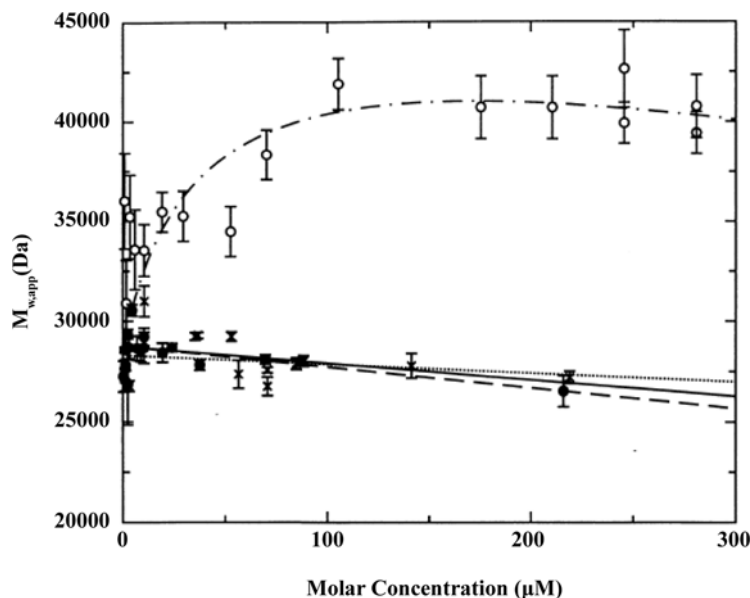
The example shown in Figure 2 [14] is again for a heterologous dimerization between molecules of similar molecular mass, in this case involving two proteins involved in molecular recognition at the cell surface: CD2 ( $M = 28.3$  kDa) and CD48 ( $M = 28.7$  kDa). A value for the second virial coefficient ( $B_{11}$ ) based on the dimensions from X-ray crystallography of  $85 \text{ \AA}$  ( $1 \text{ \AA} = 0.1 \text{ nm}$ )  $\times 23 \text{ \AA} \times 25 \text{ \AA}$  for CD2 and  $94 \text{ \AA} \times 49 \text{ \AA} \times 67 \text{ \AA}$  for CD48 and the application of the software COVOL [9,10] (<http://www.nottingham.ac.uk/ncmh/software>) yielded an average  $B_{11} = 1.8 \times 10^{-4} \text{ ml} \cdot \text{mol} \cdot \text{g}^{-2}$  and hence knowing this, from the experimental data, a value for  $K_d$  of  $\sim (1.0 \pm 0.3) \times 10^{-4}$  M was estimated, in good agreement with an estimate of

$\sim (7.5 \pm 1.5) \times 10^{-5}$  M from surface plasmon resonance. Additionally, an ISOTHERM approach (see the Sedimentation velocity section below) was also employed in this case, plotting the regression of sedimentation coefficient against  $c$ , and fitting iteratively to yield a  $K_d$  value of closely similar magnitude. In general, cases such as this, where the second virial term can be either computed or estimated, the use of software such as SEDPHAT [15] provides a simple and reliable way of securing a value for  $K_d$  and for understanding, including by 'bootstrapping', the likely levels of error present in the estimate made.

A general approach to the evaluation of (un-approximated)  $K_d$  values for weakly interacting systems (the INVEQ

**Figure 2 | Apparent weight-average molecular mass of CD2, CD48 and CD2-CD48 heterodimer as determined using SE**

×, CD2; ●, CD48; ○, CD2-CD48 heterodimer. Non-linear least-square fits to data for CD2 (dotted line), CD48 (dashed line). Continuous line: predicted regression for a value of  $2BM$  (from COVOL) of 10.4 ml/g. Dotted-dashed line: fit to CD2-CD48 data. Using the COVOL value of  $2BM = 10.4$  ml/g, a value for  $K_d \sim (1.0 \pm 0.3) \times 10^{-4}$  M is obtained, a weak interaction. With kind permission from Springer Science + Business Media: European Biophysics Journal, Characterisation of the low affinity interaction between rat cell adhesion molecules CD2 and CD48 by analytical ultracentrifugation, **25**, 1997, pp. 455-462, H. Silkowski, S.J. Davis, A.N. Barclay, A.J. Rowe, S.E. Harding and O. Byron, Figure 2.



algorithm) has recently been presented for dealing with interactions as weak as  $K_d > 5 \times 10^{-2}$  M in a pure protein system. Where the third virial term ( $3CM$ ) is significant, this can be defined in addition to the second virial term, as defined above. Even a protein so highly soluble as RNase A has been shown to self-associate in the millimolar region and to exhibit a significant third virial term under conditions of low ionic strength [16]. By analogy with the case for strong interactions presented above for the ETF system, the possible presence of irreversibly associated species still needs to be established, by either (i) several runs at different cell-loading concentration  $c^0$ , and/or (ii) a SV run to define the presence, if any, of such species. It is important that the precision of estimates of parameters secured should be defined by a full 'bootstrapping' procedure. The levels of cell loading used are critical for success, and a full definition of these levels as given by computer simulation, and of the precision which can be expected in retrieved parameters has been provided (see [16] and references cited therein).

### Sedimentation velocity

With a rotor driven at higher speeds than for SE, this method offers greater resolving power for mixtures of different components, including those in associative or dissociative equilibria, but interpretation of the records has in the past been difficult because of the contribution of hydrodynamic including shape parameters to  $c(r)$  against  $r$  profiles as they

change with time, effects which are either absent or subsumed into the thermodynamic interaction parameters in SE.

The simplest application of SV for interaction analysis is co-sedimentation, where an interaction results in a change in the sedimentation rate. The UV-absorption optical system is particularly useful in this regard and has been used, for example, to demonstrate the binding of small ligands to proteins such as the binding of adenosylcobalamin cofactor to the methylmalonyl-CoA mutase system from *Propionibacterium shermanii*: at a wavelength selected to detect the ligand only, in the presence of the mutase, all of it sediments at the same rate as the protein ( $s_{20,w}^0 \sim 7.35 \pm 0.04$  S), confirming the ligand is 100% bound [17,18]. A more spectacular example is the interaction of mepf1, a lysine-rich protein from the mussel *Mytilus edulis*, and used to help this creature adhere to surfaces, with a mucin glycoprotein. In the absence of the mucin and at a wavelength of 280 nm, the protein sediments with a  $s_{20,w}^0$  of  $2.34 \pm 0.17$  S, typical for an elongated protein of molecular mass  $\sim 110$  kDa. The addition of a small amount of mucin ( $M_w \sim 2 \times 10^6$  g/mol), at a level too low to be detected by itself at 280 nm, results in mepf1 sedimenting at 7000 S [19]. Not surprisingly, mepf1 known as 'glue protein' has been considered as a potential mucoadhesive in the biopharmaceutical industry, although the main focus of co-sedimentation as an assay for mucoadhesion has been on mucin-chitosan interactions [20].

For more subtle types of protein interaction phenomena, we need to take into account how the whole  $c(r)$  against  $r$

profiles change with time. The analogous expression to eqn (1) for SV is:

$$c(r, t) = f(f/f_0, M, k_s, k_D, K_a, r, t) \quad (6)$$

where  $f/f_0$  = the translational frictional ratio, or ratio of the friction coefficient of the protein to that for a sphere of the same volume,  $k_s$ ,  $k_D$ , are the limiting slopes of the regression of the sedimentation coefficient  $s$  or the translational diffusion coefficient  $D$  upon  $c$ .  $k_s$  can be predicted if the frictional shape of the protein is known and if the ionic strength of the supporting electrolyte is sufficiently strong to suppress polyelectrolyte effects [21]. The  $c$ -dependence of the translational diffusion coefficient ( $D$ ) involves contributions from  $k_s$  and a thermodynamic non-ideality term  $BM$  [22].

The full relationship describing the evolution of the  $c(r, t)$  profiles with  $r$  and  $t$  is a differential equation incorporating sedimentation and diffusive terms known as the Lamm equation [23] and numerical solutions are possible enabling a transformation into sedimentation coefficient distribution profiles. A great deal of recent effort has been spent dealing with the removal of contributions through time-independent noise, thus increasing the precision with which molecular parameters can be extracted. A popular algorithm for performing this transformation, which incorporates all of these advances, is the SEDFIT procedure of P. Schuck and co-workers [24,25]; this either gives a distribution uncorrected for diffusive effects, known as a  $g(s)$  against  $s$  profile, or it can give a distribution with a term correcting for this by either the user entering, or the software floating, the frictional ratio  $f/f_0$  as a parameter to yield a modified distribution known as a  $c(s)$  against  $s$  plot. Conformation information can also be used to transform this further into a molecular-mass distribution. Unfortunately, it is not yet possible to fit raw data floating all of the parameters described above; in particular, the incorporation of the total effects of concentration-dependence into Lamm equation fitting has yet to be described in experimentally useful terms. It may indeed prove to be that the number of parameters required is larger than the precision of the methodology can support.

SEDFIT is particularly good for evaluating the homogeneity/heterogeneity of a preparation. In the case of a mixture of components, it is possible to estimate the proportion of each sedimenting species present and, if there is a suspicion that they may be in a reversible equilibrium, then this can be checked by repeating an experiment at a higher loading concentration: the relative proportion of higher  $s$ -species should increase. This method has received widespread use, and has been used, for example, in the characterization of the stability and state of aggregation of antibodies in response to bioprocessing; there the higher-molecular-mass components were shown to be clearly not in a reversible equilibrium with the monomeric species [26] (Figure 3).

In terms of extracting dissociation constants, a popular approach is to use ‘sedimentation isotherms’ that is to say analyse plots of  $s_{20,w}^0$  as a function of  $c$ . Classically, in the absence of an interaction, the measured sedimentation coef-

ficient decreases with concentration owing to non-ideality effects, as represented by the  $k_s$  term. Interaction phenomena tend to reverse the trend, and one can model-fit the  $s(c)$  against  $c$  profile to estimate the stoichiometry and strength of  $K_d$  providing (i) allowance for  $k_s$  is made, and (ii) concentrations are corrected for radial dilution in the ultracentrifuge cell: the routine SC-ISOTHERM is particularly well suited to this [27]. It incorporates the extended equation for  $s$ - $c$  dependence and yields stable estimates for the  $K_a$  of an interaction, the extrapolated ( $s_0$ ) value, and the  $k_s$  value, of either the monomer alone or of both monomer and dimer. A system which possesses a reasonably narrow distribution, but is not strictly monodisperse, can be analysed without difficulty using weight-averaged  $s$  values obtained via SEDFIT. An example of this is the work on a weak reversible interaction in a carbohydrate system (a heteroxylan) [27] (Figure 4).

This approach to the study of interactions has two advantages: (i) as noted above, the ‘monomer’ can be a narrow distribution polymer rather than a monodisperse protein; (ii) it is not essential that the system is free from higher-molecular-mass components, provided that this is allowed for in the correction to true sedimenting concentration of the solute.

From the way the concentration profile in the boundary region evolves over time, it is possible to estimate the kinetics of the process, via the dissociation rate constant  $k_{off}$ ; this is limited to how fast scans can be acquired. UV-absorption optics (and also fluorescence optics) are not useful in that regard as they take  $\sim 3$  min per scan, whereas Rayleigh interference scans can be recorded every 15 s or so; a  $k_{off}$  rate higher than  $0.01 \text{ s}^{-1}$  is considered to be instantaneous, and anything lower than  $0.0001 \text{ s}^{-1}$  will not distort the boundary enough to be detected, but within this range, SV can provide reaction rate information, and has been incorporated into the program SEDANAL [28].

A comprehensive SV study has recently been conducted, showing how proteins can perform completely distinct functions depending on the particular molecules they interact with. This study, by Zhao and Beckett [29], illustrates the application of SEDFIT, SC-ISOTHERM and SEDANAL to the biotin repressor protein BirA, which switches from a homodimerization, where it serves as a transcriptional repression, to a heterodimerization, where it promotes metabolism, depending on the presence or absence of a small protein ligand known as apoBCCP87. SEDFIT was used to characterize the oligomeric state in both cases, SC-ISOTHERM was used to determine the interaction strengths or  $K_d$  values, and SEDANAL was used to determine the  $k_{off}$  for the homodimerization (Table 1).

Finally, we have already alluded to the usefulness of using sedimentation methods in conjunction with other approaches and techniques. As our final example, Walters et al. [30] have used a combination of SV in the analytical ultracentrifuge with dynamic light scattering, absorption spectrophotometry and hydrodynamic bead modelling to investigate the role of ATP in the assembly of the molecular chaperone cpn60 (GroEL14) and its co-chaperone cpn10 (GroES7) under physiologically relevant solution conditions. It was shown

**Figure 3** | Sedimentation coefficient distributions,  $g(s)$  against  $s$ , obtained using the SEDFIT algorithm for an IgG4 antibody that has undergone cycles of freeze-thaw treatment

Loading concentrations were 1.3 mg/ml in each case. The reduction of monomer species in relation to that of aggregate can be clearly seen. Adapted from [26] with permission.

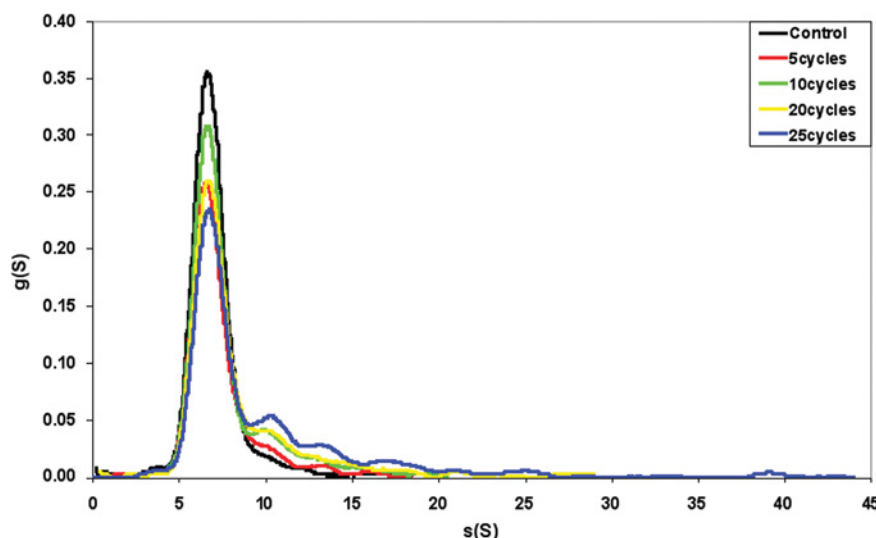
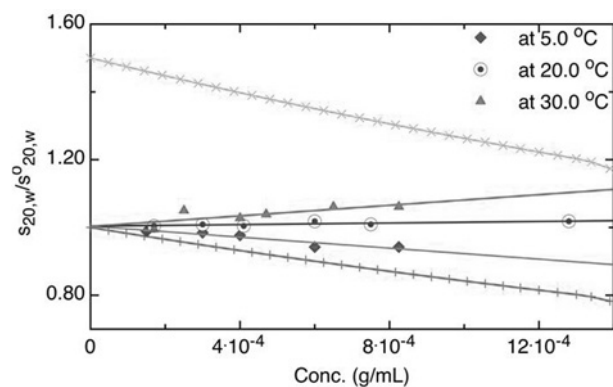


**Figure 4** | SC-ISOTHERM analysis of a heteroxylan 'PO-5', a bioactive carbohydrate, at three different temperatures

The sedimentation coefficient  $s$  is corrected to standard solvent conditions (viscosity and density of water at 20.0°C) and plotted as the ratio with the sedimentation coefficient extrapolated to  $c=0$ . A  $K_d$  of  $\sim(1.4 \pm 0.4) \times 10^{-4}$  M was obtained at 30.0°C, a value commensurate with the values obtained for cell-surface molecular-recognition interactions observed with proteins. As the temperature is decreased, the interaction becomes successively weaker, with  $K_d$  increasing to  $\sim(3.4 \pm 0.5) \times 10^{-4}$  M at 20.0°C and to almost no interaction ( $K_d > 3 \times 10^{-3}$  M) at 5.0°C. The  $\times$  symbols corresponds to the theoretical  $s$  against  $c$  dependency ( $k_s \sim 22.0$  ml/g) for a dimer and the  $+$  symbols correspond to a monomer. Adapted from [27] with permission.



that the presence of hydrolysable ATP is required to facilitate correct interaction and that non-hydrolysable ATP analogues such as adenosine 5'-[ $\gamma$ -thio]triphosphate failed to produce a measureable interaction.

**Table 1** | A molecular switch studied by sedimentation analysis

Comparative values for a homodimerization and heterodimerization of the *Escherichia coli* biotin repressor protein BirA [29]. ND, not determined.

Parameter	Value	
	In the absence of apoBCCP87	In the presence of apoBCCP87
Homodimerization* $K_d$ (M)	$(1 \pm 0.1) \times 10^{-5}$	-
Homodimerization† $k_{off}$ ( $s^{-1}$ )	$(2.7 \pm 0.5) \times 10^{-4}$	-
Heterodimerization* $K_d$ (M)	-	$(2.8 \pm 0.4) \times 10^{-6}$
Heterodimerization† $k_{off}$ ( $s^{-1}$ )	-	ND

\*from SC-ISOTHERM analysis.

†from SEDANAL.

In conclusion, we hope we have shown, within the scope of this short outline, some of the possibilities of analytical ultracentrifugation for gaining insight into the equilibria and, in some cases, dynamics of protein interactions. It has, of course, only been possible to give a few examples, but we hope that they have at least provided a representative feel spanning the range of strong to weak interactions, and also systems such as bioprocessing-induced irreversible aggregation of preparations of monoclonal antibody.

## References

- 1 Scott, D.J., Harding, S.E. and Rowe, A.J. (eds) (2005) Analytical Ultracentrifugation: Techniques and Methods, Royal Society of Chemistry, Cambridge
- 2 Creeth, J.M. and Pain, R.H. (1967) The determination of molecular weights of biological macromolecules by ultracentrifuge methods. Prog. Biophys. Mol. Biol. **17**, 217-287

- 3 Johnson, M.L., Correia, J.J., Yphantis, D.A. and Halvorson, H.R. (1981) Analysis of data from the analytical ultracentrifuge by nonlinear least-squares techniques. *Biophys. J.* **36**, 575–588
- 4 Cölfen, H., Harding, S.E., Wilson, E.K., Scrutton, N.S. and Winzor, D.J. (1997) Low temperature solution behaviour of *Methylophilus methylotrophus* electron transferring flavoprotein: a study by analytical ultracentrifugation. *Eur. Biophys. J.* **25**, 411–416
- 5 Cölfen, H. and Harding, S.E. (1997) MSTARA and MSTARI: interactive PC algorithms for simple, model independent evaluation of sedimentation equilibrium data. *Eur. Biophys. J.* **25**, 333–346
- 6 Roark, D. and Yphantis, D.A. (1969) Studies of self-associating systems by equilibrium ultracentrifugation. *Ann. N.Y. Acad. Sci.* **164**, 245–278
- 7 Wills, P.R., Jacobsen, M.P. and Winzor, D.J. (1996) Direct analysis of solute self-association by sedimentation equilibrium. *Biopolymers* **38**, 119–130
- 8 Leys, D., Basran, J., Talfournier, F., Sutcliffe, M.J. and Scrutton, N.S. (2003) Extensive conformational sampling in a ternary electron transfer complex. *Nat. Struct. Biol.* **10**, 219–225
- 9 Harding, S.E., Horton, J.C. and Winzor, D.J. (1997) COVOL: an answer to your thermodynamic non-ideality problems? *Biochem. Soc. Trans.* **26**, 737–740
- 10 Harding, S.E., Horton, J.C., Jones, S., Thornton, J.M. and Winzor, D.J. (1999) COVOL: an interactive program for evaluating second virial coefficients from the triaxial shape or dimensions of rigid macromolecules. *Biophys. J.* **76**, 2432–2438
- 11 Rallison, J.M. and Harding, S.E. (1985) Excluded volumes for pairs of triaxial ellipsoids at dominant Brownian motion. *J. Colloid Interface Sci.* **103**, 284–289
- 12 Taylor, W.R., Thornton, J.M. and Turnell, R.J. (1983) An ellipsoidal approximation of protein shape. *J. Mol. Graphics* **1**, 30–38
- 13 Reference deleted
- 14 Silkowski, H., Davis, S.J., Barclay, A.N., Rowe, A.J., Harding, S.E. and Byron, O. (1997) Characterisation of the low affinity interaction between rat cell adhesion molecules CD2 and CD48 by analytical ultracentrifugation. *Eur. Biophys. J.* **25**, 455–462
- 15 Vistica, J., Dam, J., Balbo, A., Yikilmaz, E., Mariuzza, R.A., Rouault, T.A. and Schuck, P. (2004) Sedimentation equilibrium analysis of protein interactions with global implicit mass conservation constraints and systematic noise decomposition. *Anal. Biochem.* **326**, 234–256
- 16 Ang, S. and Rowe, A.J. (2010) Evaluation of the information content of sedimentation equilibrium data in self-interacting systems. *Macromol. Biosci.*, doi:10.1002/mabi.201000065
- 17 Marsh, N. and Harding, S.E. (1993) Methylmalonyl-CoA mutase from *Propionibacterium shermanii*: characterization of the cobalamin-inhibited form and subunit-cofactor interactions studied by analytical ultracentrifugation. *Biochem. J.* **290**, 551–555
- 18 Harding, S.E. and Winzor, D.J. (2000) Sedimentation velocity analytical ultracentrifugation. in *Protein-Ligand Interactions: Hydrodynamics and Calorimetry* (Harding, S.E. and Chowdhry, B.Z., eds), pp. 75–103, Oxford University Press, Oxford
- 19 Deacon, M.P., Davis, S.S., Waite, J.H. and Harding, S.E. (1998) Structure and mucoadhesion of mussel glue protein in dilute solution. *Biochemistry* **37**, 14108–14112.
- 20 Harding, S.E. (2003) Mucoadhesive interactions. *Biochem. Soc. Trans.* **31**, 1036–1041
- 21 Rowe, A.J. (1992) The concentration dependence of sedimentation. in *Analytical Ultracentrifugation in Biochemistry and Polymer Science* (Harding, S.E., Rowe, A.J. and Horton, J.C., eds), pp. 394–406, Royal Society of Chemistry, Cambridge
- 22 Harding, S.E. and Johnson, P.J. (1985) The concentration dependence of macromolecular parameters. *Biochem. J.* **231**, 543–547
- 23 Lamm, O. (1929) Die Differentialgleichung der Ultrazentrifugierung. *Ark. Mat. Astron. Fys.* **21B**, 1–4
- 24 Dam, J., Velikovsky, C.A., Mariuzza, R.A., Urbanke, C. and Schuck, P. (2005) Sedimentation velocity analysis of heterogeneous protein-protein interactions: Lamm equation modeling and sedimentation coefficient distributions  $c(s)$ . *Biophys. J.* **89**, 619–634
- 25 Schuck, P. (2010) Sedimentation patterns of rapidly reversible protein interactions. *Biophys. J.* **98**, 2005–2013
- 26 Lu, Y., Harding, S.E., Rowe, A.J., Davis, K.G., Fish, B., Varley, P., Gee, C. and Mulot, S. (2008) The effect of a point mutation on the stability of IgG4 as monitored by analytical ultracentrifugation. *J. Pharm. Sci.* **97**, 948–957
- 27 Patel, T.R., Harding, S.E., Ebringerova, A., Deszczynski, M., Hromadkova, Z., Togola, A., Paulsen, B.S., Morris, G.A. and Rowe, A.J. (2007) Weak self-association in a carbohydrate system. *Biophys. J.* **93**, 741–749
- 28 Stafford, W.F. and Sherwood, P.J. (2004) Analysis of heterologous interacting systems by sedimentation velocity: curve fitting algorithms for estimation of sedimentation coefficients, equilibrium and rate constants. *Biophys. Chem.* **108**, 231–243
- 29 Zhao, H. and Beckett, D. (2008) Kinetic partitioning between alternative protein-protein interactions controls a transcriptional switch. *J. Mol. Biol.* **380**, 223–226
- 30 Walters, C., Errington, N., Rowe, A.J. and Harding, S.E. (2002) Hydrolysable ATP is a requirement for the correct interaction of molecular chaperonins cpn60 and cpn10. *Biochem. J.* **364**, 849–855

---

Received 11 May 2010  
doi:10.1042/BST0380901